51st International Conference on Environmental Systems
10-14 July 2022, St. Paul, Minnesota ICES-2022-357

Experiments on a Loop Heat Pipe with a 3D Printed Evaporator

Rohit Gupta[1], Chien-Hua Chen[2], and William G. Anderson[3]
Advanced Cooling Technologies, Inc. Lancaster, PA, 17601

The construction and testing of a loop heat pipe with a 3D printed evaporator is described in this paper. The system was developed as part of a larger engineering demonstration unit for thermal management on NASA's Volatiles Investigating Polar Exploration Rover. A state-of-the-art 3D printed evaporator, developed in a previous effort, was used in the current system. This evaporator had a cylindrical geometry with a length of 0.1 m and a diameter of 0.025 m and featured a primary wick with a bubble point pore radius of under 8 µm. The vapor, condenser, and liquid lines were constructed from 0.003 m diameter tubing and routed to conform to the geometry of the rover. A thermal control valve was also incorporated in the loop heat pipe to force the vapor to bypass the condenser at a lower-than-threshold temperature. The loop heat pipe was tested successfully under a range of thermal loads of up to 70 W against a mission-expected load of 50 W. Due to startup difficulties observed at the low condenser temperatures, a series of dedicated startup tests were conducted to identify the underlying causes and to study the effects of major variables, such as the heat location and charge quantity. Based on this analysis, a number of changes were identified to help improve the startup performance of the system.

Nomenclature

C	=	conductance (in W/ºC)
d	=	diameter (in m)
l	=	length (in m)
P	=	power (in W)
r	=	radius (in µm)
T	=	temperature (in ºC)

I. Introduction

THE rapid growth in the use of spacecraft for science and commerce has created increased demand for low-cost heat transfer devices. A Loop Heat Pipe (LHP) is particularly suited for spacecraft applications as the system is capable of transferring heat over large distances with very high conductance owing to the two-phase nature of the system. Unlike a traditional heat pipe, a LHP features a smooth-wall condenser which can more easily be installed on deployable radiators. However, LHPs have a high manufacturing cost due to the intensive labor demands associated with fabricating a primary wick, incorporating vapor grooves, and achieving a sealed wick-envelope integration. As such, ACT has been conducting a long-term campaign to develop 3D printed evaporators for LHPs as part of several NASA SBIR programs. With 3D printing, the evaporator can be created directly from the machine as a single, continuous part, complete with such features as the primary wick, vapor grooves, and a solid outer wall, leading to significant cost and time savings. Prior to the current development, ACT's work on 3D printed evaporators has primarily been aimed at improving the capillary performance of the primary wick, as described in the literature.[1–3] Most notably in these previous efforts, ACT was able to significantly improve the wick capillary limit to a level that corresponds to a bubble-point pore radius of under r = 5 µm.

The current paper, however, describes the construction and testing of a LHP designed to a set of prescribed mission requirements and featuring the current state-of-the-art 3D printed evaporator developed by ACT. The LHP under

---

[1] R&D Engineer II, 1046 New Holland Avenue, Lancaster, PA 17601.
[2] R&D Manager, 1046 New Holland Avenue, Lancaster, PA 17601.
[3] Chief Engineer, 1046 New Holland Avenue, Lancaster, PA 17601.

discussion was developed as part of a larger engineering demonstration unit for thermal management on NASA's Volatiles Investigating Polar Exploration Rover (VIPER). The VIPER mission aims to land a rover at the south pole of the moon with the objective of mapping the distribution and composition of lunar ice for future human space exploration. Given the novelty of 3D printed evaporators, one of the goals of testing was to find and diagnose any potential issues with the LHP for future corrections. It should be highlighted that to the best of the authors' knowledge, this work describes the first instance of the design, fabrication, and testing of a mission-specific LHP with a 3D printed evaporator, thereby advancing its technological readiness level in the process.

II. Construction

The LHP was designed to the constraints imposed by the geometry of VIPER, with the goal of collecting heat from the VIPER's spectrometers and rejecting it to one of the overhead radiator panels. A CAD rendering of the LHP is presented in Figure 1 (left) with a magnified image of the evaporator area shown in inset. The 3D printed evaporator used in the current system represents the best iteration from the previous developmental work on this component.[3] A CAD rendering of the evaporator cross-section, with the various highlighted regions, is presented in Figure 2 (top). A photograph of the evaporator, printed from 316 L SS powder using laser powder bed fusion, is also presented in Figure 2 (bottom). The evaporator was designed with a simple cylindrical geometry having a length of $l \approx 0.1$ m and a diameter of $d \approx 0.025$ m.

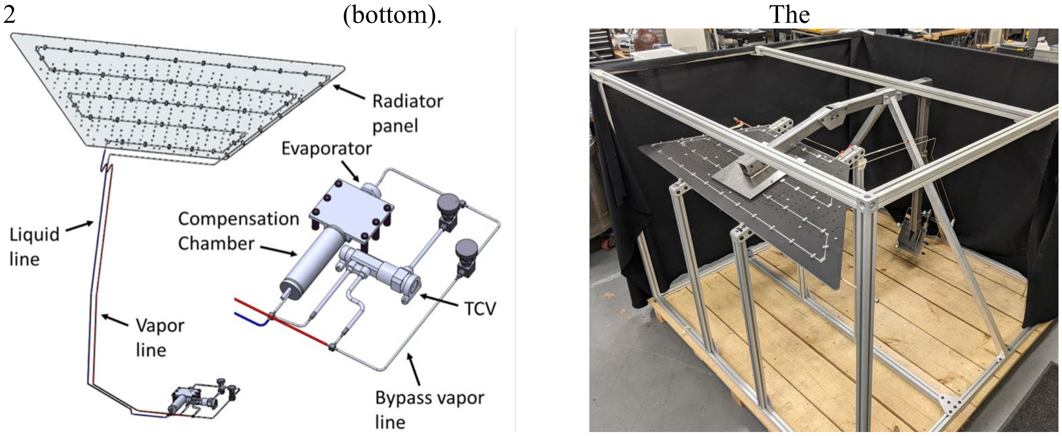

Figure 1. A CAD rendering of the LHP developed by ACT with a magnified view of the evaporator region in inset (left), and a photograph of the LHP installed in the shipping rack at ACT (right).

The capillary parameters for the evaporator primary wick are listed in Table 1. Most notably from Table 1, the 3D printed wick was associated with an equivalent pore radius, measured at bubble point, of under $r = 8$ μm. A physical interpretation of this radius can be obtained by visualizing the wick coupon as a collection of isolated voids and complicated connected paths that allow for the transport of fluid in response to an external pressure gradient. As the 3D printed wick doesn't have a well-defined lattice structure, the connected paths can be logically reasoned to have non-uniform cross-sections, with complex variations in the cross-sectional area expected along any given path. Moreover, the minimum and maximum cross-sectional areas are also expected to be different for different paths. In this visual framework, the bubble-point radius corresponds to the largest of the minimum cross-sectional areas of the connected paths in the sample.

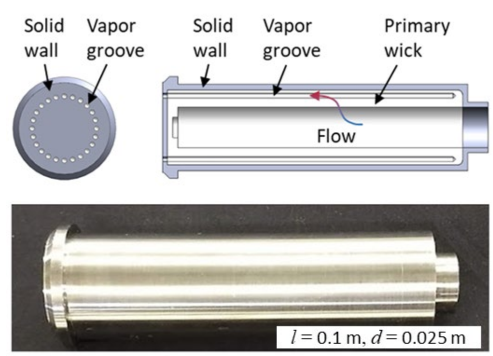

Figure 2. A CAD rendering of the 3D printed evaporator (top), and a picture of the printed evaporator (bottom).

A Thermal Control Valve (TCV) was incorporated in the vapor line, as seen in Figure 1 (left), to direct the vapor along a bypass path, free of the condenser, at a lower-than-threshold temperature. A second vapor line, without a TCV, was also included in the design, see Figure 1 (left), to allow for the isolated testing of the LHP before using the system with the TCV. A photograph of the LHP installed in the shipping rack prior to being delivered to NASA is shown in Figure 1 (right). The reflux arrangement in Figure 1 (right) closely resembles the expected real arrangement of the system on VIPER. An important detail of the current configuration is the position of the evaporator below the compensation chamber, which results in the flooding of the evaporator with sub-cooled liquid prior to startup. This configuration was chosen to ensure an uninterrupted supply of liquid to the evaporator during LHP operation. However, the flooding of the evaporator prior to startup was found to have a significant impact on the test results, as detailed in Section III. The dimensions of the major LHP components are presented in Table 2. The vapor, condenser, and liquid lines were constructed from tubing with a small diameter of d = 0.003 m in order to minimize the quantity of the working fluid and reduce the overall weight of the system. The radiator panel was fabricated from Al6061 and featured a grooved path for the condenser line to try and maximize the area of contact for better thermal conductance of the system.

Table 1. Parameters of the primary wick region in the 3D printed evaporator

Parameter	Value
Material	316L SS
Pore radius	7.6 µm
Porosity	29%
Permeability	1.16×10^{-13} m^2

Table 2. Dimensions of the major components of the NASA VIPER LHP

Parameter	Value
Evaporator:	
Diameter	0.025 m
Length	0.1 m
Compensation Chamber:	
Diameter	0.038 m
Length	0.13 m
Fluid Lines:	
Diameter	0.003 m (outer), 5×10^{-4} m (thick)
Vapor line length	3 m
Condenser line length	6 m
Liquid line length	2 m
Radiator:	
Area	0.525 m^2

III. Results

A. LHP Testing

A series of tests were conducted at ACT with the LHP in reflux mode, as would be expected during real operation. Propylene was used as the working fluid in the system due to the low freezing point, which makes it suitable for lunar applications. Some temperature profiles from a test conducted via the second vapor line, free of the TCV, with an intended condenser temperature of T_C = 0 ºC are presented in Figure 3. In this figure, the LHP is seen to operate under a range of thermal loads between P = 20 W and P = 70 W at a near flat conductance of C = 5.5 W/ºC. This conductance is calculated following a global definition that is based on the difference in temperatures at the evaporator and the cold plate. The primary factor affecting the system conductance is the inadequate insulation around the liquid line leading to a large temperature jump between the exit of the condenser and the inlet of the compensation chamber of over ΔT = 4 ºC. An additional contribution stems from the temperature difference between the cold plate and the condenser. Due to inadequate thermal contact, the actual temperature of the condenser during testing was several degrees higher than the intended temperature of T_C = 0 ºC. The various contributing factors affecting the system conductance were not actively addressed as the goal of these tests wasn't to optimize the system conductance but to merely conduct a trial run of the LHP before delivery to NASA. One noteworthy observation from Figure 3 is the successful operation of the LHP at P = 70 W,

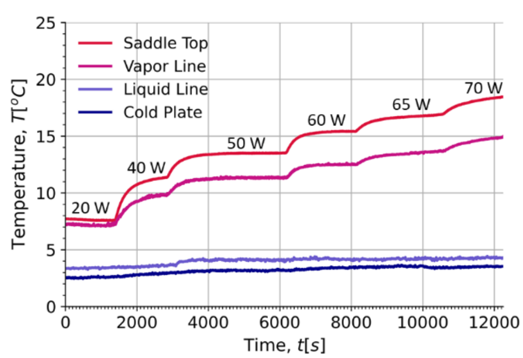

Figure 3. Temperature profiles corresponding to the LHP operation at an intended condenser temperature of T_c = 0 ºC.

which is 20 W greater than the expected thermal load of P = 50 W during intended operation. It should be highlighted that despite a seemingly low thermal load, the total pressure drop being overcome by the evaporator during operation at P = 70 W is expected to be quite significant due to the combination of small tubing diameter and long fluid lines of the LHP. An additional observation of interest during these tests was the difficulty in effecting LHP startup at the lower condenser temperatures, requiring increasingly higher thermal loads with greater cooling of the condenser. In order to understand the underlying physics of this behavior, a set of dedicated startup tests were conducted at ACT, as described in the following section.

B. Startup Testing

Since the LHP had to be shipped to NASA for thermal-vacuum testing, the startup tests were conducted on a modified version of the ACT LHP test rig, introduced previously in the literature[3]. The modification to the test rig involved rearranging the evaporator and compensation chamber to be consistent with the shipped LHP, as described in Section II. Thus, with the test rig in an equivalent reflux position, the evaporator is completely flooded with sub-cooled liquid prior to startup. For additional equivalence, the LHP test rig featured a spare 3D printed evaporator with a capillary performance that is comparable with that in Table 2. Propylene was also used as the working fluid for these tests.

Effect of heat location

The objective with the first set of tests was to study the effect of heat location on LHP startup. Figure 4 shows a schematic of the evaporator and compensation chamber along with the approximate locations of the embedded cartridge heaters, numbered 1 – 4, that were used for heating of the evaporator saddle. LHP startup was first attempted with top heating using heaters 1 and 2 at a range of condenser temperatures between T_C = -120 ºC and T_C = -15 ºC. Thereafter, startup was attempted with bottom heating from the remaining two heaters with identical power and condenser settings. A comparison of the startup behavior from top and bottom heating with a constant thermal load of P = 40 W and a condenser temperature of T_C = -15 ºC is presented in Figure 5. For both the cases in Figure 5, the initial state of the system before heat application is characterized by a liquid line temperature that is greater than the vapor line temperature, indicating reverse movement of fluid through the LHP. In order to explain this behavior, it is important to note the state of the fluid within the LHP prior to the cooling of the condenser. Upon charging of the LHP, the liquid in the system assumes a constant height with liquid-vapor interfaces appearing in the compensation chamber, liquid, and vapor lines. At the start of the cooling process, the temperature in the vapor line falls more rapidly than the liquid line as the coolant enters in the vicinity of the former and exits near the latter, following a pre-arranged serpentine path on the surface of the cold plate. The difference between the temperatures and the corresponding saturation pressures therefore causes the fluid to move in reverse, similar to a loop thermosyphon. For successful forward operation of the LHP, the applied heat must result in vaporization of the fluid in the evaporator, creating a two-phase interface that is required for capillary locking.

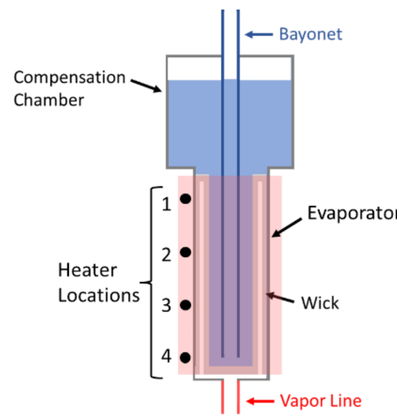

Figure 4. A schematic of the evaporator and compensation chamber of the LHP.

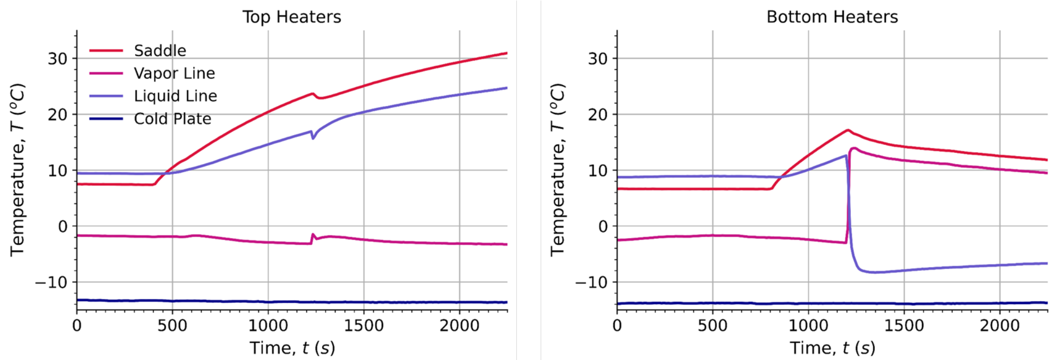

Figure 5. Temperature profiles corresponding to LHP startup attempts with top heating (left) and with bottom heating (right) with a thermal load of P = 40 W and at a condenser temperature of T_c = -15 ºC.

With top heating, the liquid and vapor line temperatures, from Figure 5 (left), continue to diverge except for an intermittent blip, indicating a failure in sustaining vapor generation in the wick. This general observation remains independent of the condenser temperature, indicating LHP startup failure with top heating up to a power of P = 100 W, which was the highest setting used in the current tests. However, bottom heating in Figure 5 is observed to force a crossover of the liquid and vapor line temperatures after a period of time, indicating successful startup of the LHP. Moreover, this startup success is observed across the entire range of condenser temperatures, in stark contrast with the case with top heating. The disparity in the LHP startup can be explained by recognizing that the proximity to the heat location with top heating leads to a more rapid growth in the temperature and saturation pressure inside the compensation chamber as compared to bottom heating. As such, top heating causes an enhancement of the LHP reverse flow rather than achieve sustained vaporization in the primary wick, leading to the observed startup failure. This problem, however, can be mitigated by pursuing an alternative arrangement with the compensation chamber positioned below the evaporator to prevent complete flooding of the evaporator with sub-cooled liquid prior to the application of heat. A fine secondary wick can be employed in this alternative arrangement to supply liquid from the compensation chamber to the evaporator against the force of gravity.

Effect of charge quantity

As mentioned in the previous section, the LHP was started successfully with bottom heating at a range of condenser temperatures between T_C = -120 ºC and T_C = -15 ºC. The thermal loading required for startup, however, was seen to increase with decreasing condenser temperature, as shown in Figure 6. This dependency is a direct reflection of the greater subcooling of liquid inside the evaporator due to a decrease in the average LHP temperature with increased condenser cooling. As an example, Figure 7 compares the startup behavior at two different condenser temperatures of T_C = -15 ºC and T_C = -30 ºC with a fixed thermal load of P = 30 W. From Figure 7, a successful startup is only observed at the higher condenser temperature with only a sustained reverse operation observed at the lower temperature.

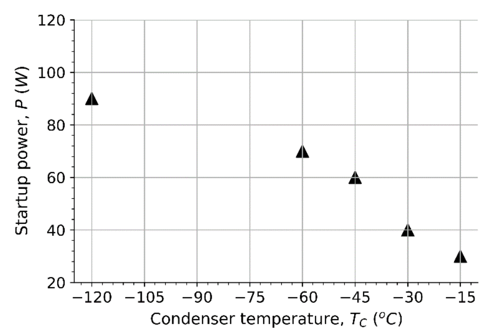

Figure 6. Variation in the startup power with condenser temperature.

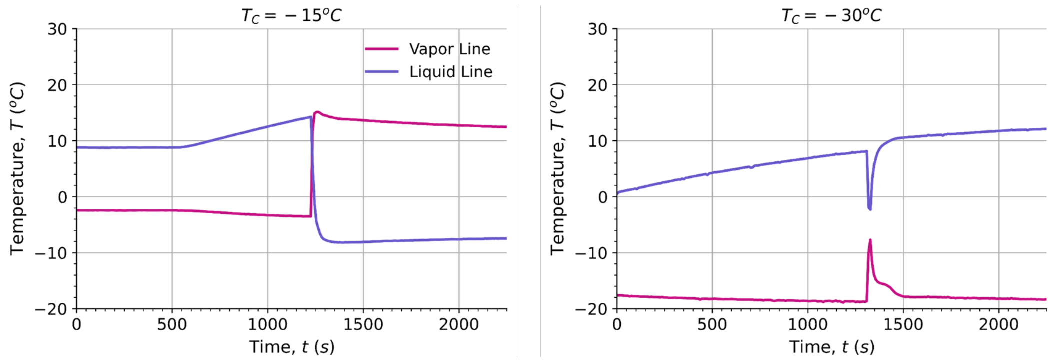

Figure 7. Temperature profiles corresponding to the LHP startup attempts with a thermal load of P = 30 W at two different condenser temperatures of T_c = -15 °C (left) and T_c = -30 °C (right).

A second set of startup tests was conducted with the objective of understanding the effect of charge quantity on the startup behavior. The startup results presented thus far were acquired with the LHP charged with 115 g of propylene. This charge quantity was derived following the standard charge calculation process in the literature,[4] which is designed to ensure liquid in the evaporator during cold startup and sufficient space in the compensation chamber for the accumulation of liquid during hot operation. For these additional startup tests, the charge quantity was first increased to 195 g and then to 275 g, with the latter corresponding to a state in which the compensation chamber is also fully flooded with liquid during startup between condenser temperatures of T_C = -60 °C and T_C = -30 °C. Figure 8 shows a comparison of the startup power dependance on the condenser temperature at three different charges. An increase in the propylene charge is seen from Figure 8 to lead to a general flattening of the startup power curve, with the highest charge case showing complete independence to the condenser temperature between T_C = -45 °C and T_C = -15 °C. Thus, with a heavier charge, the results indicate an easier startup at the lower end of the temperature range and a more difficult startup at the higher end. For additional emphasis, the startup data for the 115 g and the 275 g cases are compared in Figure 9 and Figure 10. The data in Figure 9 and Figure 10 were acquired under different thermal loads of P = 40 W and P = 60 W, and at different condenser temperatures of T_C = -30 °C and T_C = -60 °C, respectively. At the higher condenser temperature, the crossover in the liquid and vapor line temperatures can only be seen in the 115 g case. In contrast, with the condenser cooled down to T_C = -60 °C, it is the 275 g case that shows the characteristic temperature crossover that is indicative of successful startup of the LHP.

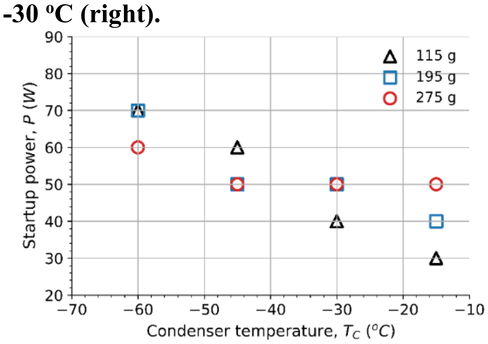

Figure 8. The dependance of startup power on condenser temperature at three different propylene charges.

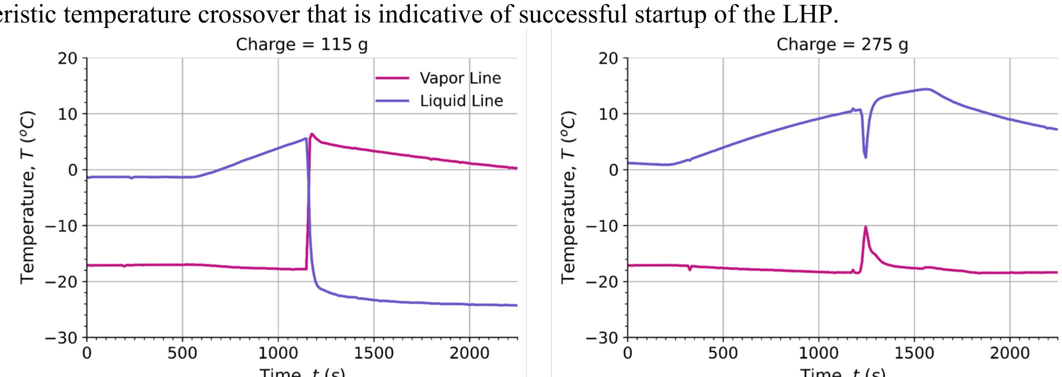

Figure 9. Temperature profiles corresponding to the LHP startup attempts with two different charges of 115 g (left) and 275 g (right) under a constant thermal load of P = 40 W and condenser temperature of T_c = -30 °C.

The results from Figure 8 can be understood by revisiting the behavior of the system during the cool down of the condenser. With standard charge of 115 g, a liquid-vapor interface appears in the compensation chamber and the liquid line, as had been indicated previously. During cooling of the condenser for testing, the liquid in the compensation chamber begins to drain into the liquid line in response to the pressure gradient set up by the instantaneous temperature difference in the respective saturation states. This phenomenon leads to a rise in the liquid column in the liquid line, which in turn creates additional pressure head leading to greater subcooling of the liquid in the evaporator. Thus, the steepness of the power curve in Figure 6 is a result of increasingly sub-cooled liquid due to a combination of decreasing average temperature and increasing pressure head. For the case with 275 g of propylene, the compensation chamber is completely flooded with sub-cooled liquid, as had been indicated before, with the liquid-vapor interface appearing further up along the liquid line. Thus, due to a high initial liquid column, the threshold for startup at the higher end of the condenser temperature range, such as in Figure 9, is greater than the standard charge case. However, without compressible vapor, the liquid in the compensation chamber is expected to drain minimally in response to the cooling of the condenser, leading to a near-constant liquid column height in the liquid line. Without a growing pressure head, the startup power shows a weaker dependance on the condenser temperature, leading to a reduced startup threshold at the lower condenser temperatures, as was the case in Figure 10. Therefore, as a future recommendation, LHPs of the current configuration should be charged to ensure complete flooding of the compensation chamber for easier startup at low condenser temperatures, as could be expected in a lunar environment.

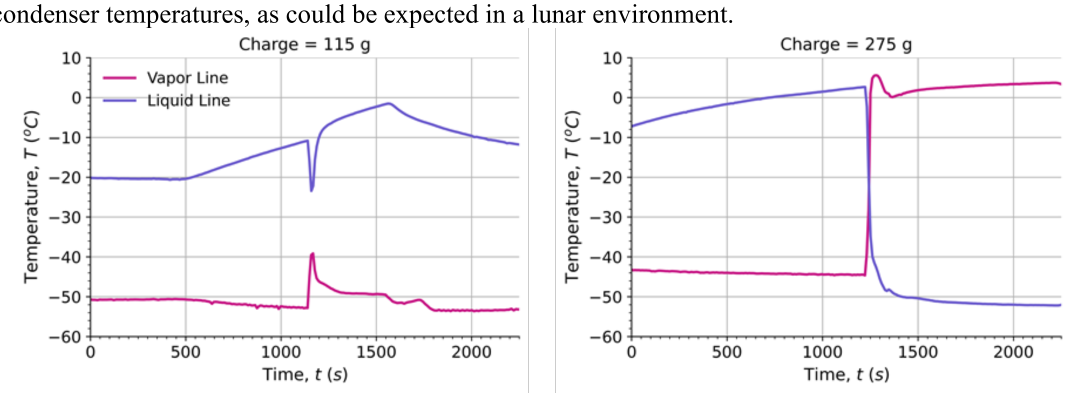

Figure 10. Temperature profiles for the LHP startup attempts with two different charges of 115 g (left) and 275 g (right) under a constant thermal load of *P* = 60 W and condenser temperature of T_c = -60 °C.

IV. Conclusion

A LHP with a 3D printed evaporator was developed by ACT as part of a larger engineering demonstration unit for NASA's VIPER. The system was motivated by the need to efficiently transfer heat from VIPER's scientific instruments to the radiator. The 3D printed evaporator featured a primary wick with a sub 8 µm pore radius at bubble point and was developed as part of a separate NASA-funded effort. The overarching objective of this work was to demonstrate the operational success of a mission-specific LHP with a 3D printed evaporator. This demonstration formed part of an ongoing effort by ACT to raise the technological readiness level of 3D printed evaporators and other additively-manufactured LHP components. Against an expected thermal load of *P* = 50 W, the ACT LHP was operated successfully up to a power of *P* = 70 W. A series of dedicated startup tests were also conducted due to the LHP startup difficulties noted at the lower condenser temperatures. These difficulties stemmed from the arrangement of the evaporator below the compensation chamber, which in reflux operation, resulted in the complete flooding of the evaporator with sub-cooled liquid prior to startup. The effects of various parameters, such as heat location, condenser temperature, and charge quantity were studied as part of the startup tests to help gain a robust understanding of the underlying physical mechanisms. Following the analysis of the startup results, several recommendations were outlined, aimed at enhancing vaporization in the evaporator for easier startup of the LHP.

Acknowledgments

This work was funded by NASA through the Small Business Innovation Research (SBIR) program under contracts 80NSSC21C0563 and NNX17CM09C.

References

[1]Richard, B., Pellicone, D., and Anderson, W.G., "Loop Heat Pipe Wick Fabrication via Additive Manufacturing," *Proceedings of the 48th Internation Conference on Environmental Systems*, Albuquerque, New Mexico, 2018.

[2]Richard, B., Anderson, W.G., Chen, C-H., Crawmer, J., and Augustine, M., "Development of a 3D Printed Loop Heat Pipe," *Proceedings of the 49th International Conference on Environmental Systems*, Boston, Massachussets, 2019.

[3]Gupta, R., Chen, C-H., and Anderson, W.G., "Progress on 3D Printed Loop Heat Pipes," *Proceedings of the 50th International Conference on Environmental Systems,* Virtual, 2021.
[4]Ku, J., Operating characteristics of loop heat pipes, *SAE transactions*, 1999, pp.503-519.